Engineering Geology 177 (2014) 10–24

Contents lists available at ScienceDirect

Engineering Geology

journal homepage: www.elsevier.com/locate/enggeo

Rapid channelization and incision into soft bedrock induced by human activity — Implications from the Bachang River in Taiwan

Ming-Wan Huang [a], Jyh-Jong Liao [a,*], Yii-Wen Pan [a], Meng-Hsiung Cheng [a,b]

[a] Department of Civil Engineering, National Chiao Tung University, 1001, University Road, Hsinchu 30010, Taiwan
[b] Water Resources Planning Institute, Water Resources Agency, MOEA, 1340, Jhong-jheng Road, Wu-fong, Taichung 41350, Taiwan

ARTICLE INFO

Article history:
Received 30 October 2013
Received in revised form 7 May 2014
Accepted 10 May 2014
Available online 17 May 2014

Keywords:
River morphology
Human influence
Soft rock
Bachang River
Taiwan

ABSTRACT

Many Taiwanese river channels have been affected by human activity, such as engineering works and gravel mining. Environmental conditions such as high seasonal precipitation and young sedimentary bedrock exaggerate the narrowing and incising of river channels. The Bachang River is located in southwestern Taiwan, and the 11-km-long channel at its midstream reach has been incised to a maximum depth of approximately 30 m within several decades. Therefore, the morphologic evolution of the Bachang River in southwestern Taiwan provides an illustration of channel changes in response to human activity. The historical data used for this analysis of morphology change include one set of topographic maps and six sets of aerial photographs from the past 100 years. The channel changes are analyzed qualitatively and quantitatively and include the channel planform, longitudinal profiles, channel incision, channel width, and channel cross sections. The results indicate that remarkable channel changes have occurred since the 1980s as a result of human influence. The 11-km-long study reach transformed from an alluvial-type channel to a gorge-type channel within several decades. The maximum accumulated depth of the channel incision is approximately 30 m, with a meter-scale annual average incision rate; the maximum width has been decreased to approximately one-sixth of the original width (448 m). The process of channel evolution is divided into four stages, and we have concluded that the causes of channel change include six factors from two categories: natural factors that include geological conditions, hydrological conditions, and the process of bedrock erosion; and human factors that include gravel mining, lateral structures, and levees. The initiation of channel evolution is triggered by human factors. Finally, we discuss the potential future channel evolution and lessons learned from the case study.

1. Introduction

The morphology of river channels may change in response to human activity and various natural influences. Human intervention may include activities such as dam construction, gravel mining, flow diversion, levee construction, water extraction, and infrastructure construction. The consequences of human impacts include disturbances to stream gradations, which induce an adjustment in the channel geometry and gradient to a new equilibrium. The construction of dams may trap sediment and regulate flow discharge downstream, causing scour below the dam and a reduction in channel capacity (Kondolf, 1997). Gravel mining activity may cause knickpoint migration upstream of the mining pit and induce incisions downstream (Kondolf, 1994). Flow diversion and water extraction decrease the river discharge and may induce channel aggradation. Levee and embankment construction may increase the flow velocity and induce scour around bridge piers at bridge crossings (Gregory, 2006). However, the channel morphology changes with respect to various processes are accumulated spatially and temporally (Reid, 1993). The channel adjustments are not always predictable because of the complex responses from diverse hydraulic and geological conditions.

Without human influence, alluvial streams may change continually between degradation and aggradation in graded conditions (Lane, 1955). Once a river system process is altered by human activity, other processes change in compensation. Numerous examples of river–channel evolution as a result of human influence have been studied worldwide to enhance the understanding of the effects of human impacts on channel adjustments. Channel incision and narrowing are the two main types of channel adjustments in response to human disturbances that are recognized in Italy (Surian and Rinaldi, 2003); deforestation and clearance have caused the sediment supply to increase, which is an early trend (the earliest was in Roman times and major phases occurred in the 18th to 19th centuries) in the Mediterranean region. However, recent trends have demonstrated the adverse effects of damming and river controls on incised channels (Hooke, 2006), and significant channel incision and narrowing has been caused by flood

* Corresponding author. Tel.: +886 3 5712121x54939; fax: +886 3 5724125.
E-mail address: jjliao@mail.nctu.edu.tw (J.-J. Liao).

http://dx.doi.org/10.1016/j.enggeo.2014.05.002
0013-7952/

embankments and grade control structures in the downstream reaches of the lower Santa Clara River (Downs et al., 2013). In recent decades, extensive channel narrowing in south-eastern France has been demonstrated to be related to human controls (Liebault and Piegay, 2002). Human influence has an overwhelming effect on fluvial geomorphologic changes, and additional research should focus on understanding the future trends of channel evolution for river management.

Bedrock or mixed bedrock-alluvial channels, unlike alluvial channels, retain resistant flow boundaries with a high erosion threshold. Channel incisions in bedrock channels may be hindered (Zawiejska and Wyzga, 2010) because of the slow rate of bedrock erosion (Tinkler and Wohl, 1998; Stock et al., 2005). However, the erosion rate in soft bedrock rivers may be rapid and dominate the evolution of channel morphology (Lai et al., 2011; Huang et al., 2013b; Liao et al., 2013). The characteristics of soft bedrock channels in response to human influences may provide valuable information on the geological factors that affect river behavior.

Taiwan is a spindle-shaped island with a short axis in an east–west direction and maximum length of approximately 140 km (Figure 1A). The Central Mountain Range (highest elevation of approximately 4000 m asl) crosses the island in a north–south direction and is the principal hydrological divide of Taiwan. Topographically, the major streams of Taiwan headwater in the Central Mountain Range flow typically in an east–west direction; therefore, the majority of stream lengths do not exceed 100 km. The annual average precipitation in Taiwan is over 2500 mm, but precipitation levels are concentrated in the wet season from May to October. The stream discharge is highly seasonal and flows rapidly through short and steep channels into the sea. Consequently, many engineering works have been constructed in streams for flood control and water resources. Major flow regulation works, which were primarily constructed from the 1960s to 1970s, have influenced the channel morphodynamics. Bridges and erosion control works are other major causes of channel disturbance. Moreover, instream gravel mining has been considered an economical source of construction material. Human disturbance has significantly modified the nature and rate of river adjustments by altering the spatial and temporal distribution of river forms and processes.

In this paper, the Bachang River in southwestern Taiwan is used to demonstrate the channel morphologic changes that result predominantly from human activity. The human influences are composed sequentially of gravel mining, bridge construction, and weir installation. These interventions on the river bed have triggered a severe bedrock incision of the Bachang River. A series of drop structures have been constructed on the riverbed as countermeasures to protect the bed from channel degradation. However, the exposed soft bedrock is prone to erosion without the armor-layer protection; consequently, the channel morphology has continuously changed toward a gorge-type channel. A comparison of one set of topographic maps and six sets of aerial photographs from the past 100 years has revealed the process of human influence and channel narrowing. The channel change processes are compared temporally and spatially using plane geometries, longitudinal profiles, cross-section geometries, and average channel widths. The possible causes of channel narrowing and deepening are addressed and summarized with respect to natural conditions and anthropogenic influences. Finally, future potential channel evolution and the lessons learned from the case study are discussed.

2. The site location and background

The Bachang River drains approximately 475 km^2 with an elevation ranging from approximately 1940 m in the Fenchihu Mountain to sea level at the estuary in southwestern Taiwan (Figure 1). The total trunk

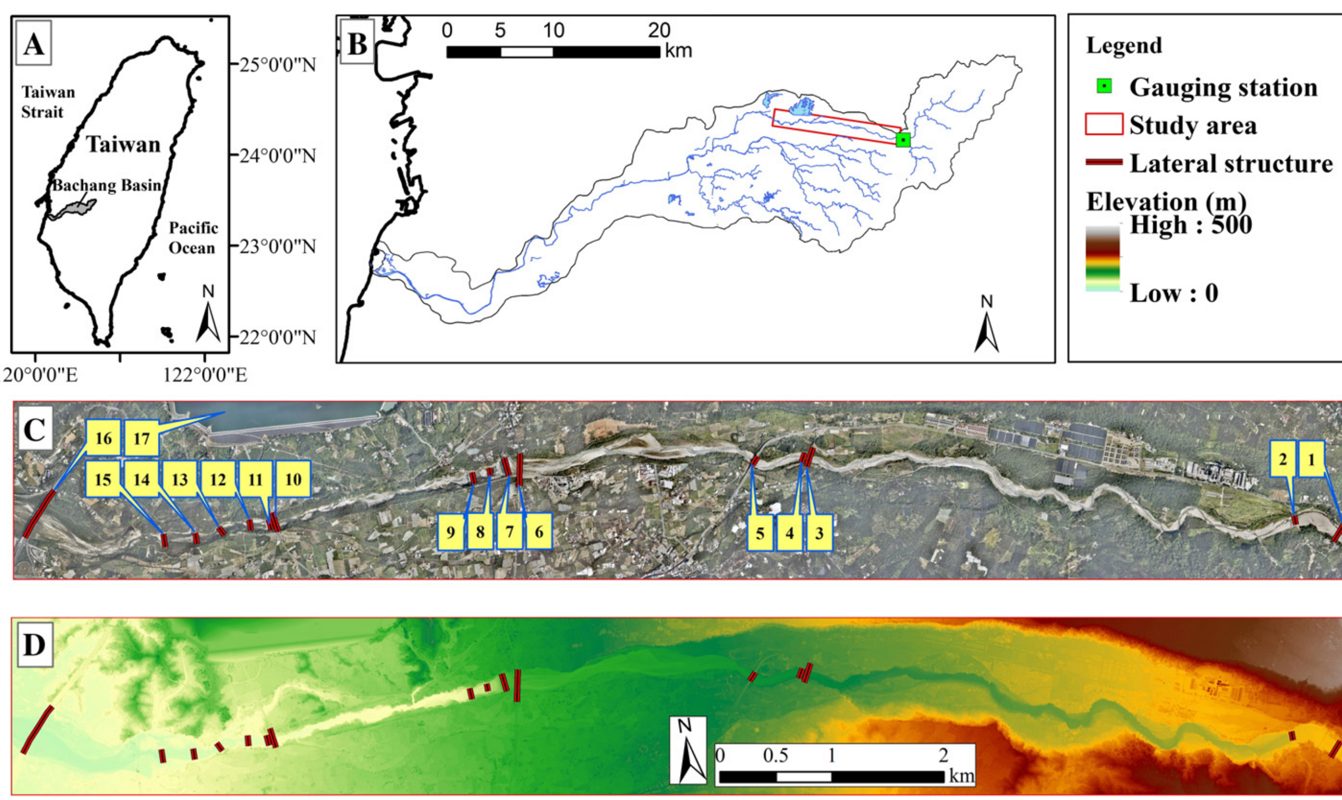

Fig. 1. Location maps of the study reach. (A) The Bachang River location in southwestern Taiwan. (B) The location of the study reach in the Bachang River. (C) The aerial orthophoto of the study reach in 2012. (D) The digital surface model of the study reach in 2012. Flow direction is from right to left. The red thick lines denote the locations of the lateral structures, which include six bridges (Nos. 1, 3, 5, 6, 10, and 16), two weirs (Nos. 2 and 7), and eight drop structures (Nos. 4, 8 and 9, and 11 to 15). The structure names are as follows: 1) Hsingyuan Bridge; 2) Chukou Weir; 3) Wuhuliao Bridge; 4) Drop structure of Wuhuliao Bridge; 5) New Wuhuliao Bridge; 6) Wufeng Bridge; 7) Renyitan Weir; 8) Drop structure No. 18; 9) Drop structure No. 17; 10) Renyitan Bridge; 11) Drop structure No. 7; 12) Drop structure No. 6; 13) Drop structure No. 5; 14) Drop structure No. 4; 15) Drop structure No. 3; 16) Freeway Bridge; and 17) Renyitan Reservoir.

length of the Bachang River is approximately 81 km. The study reach, which is approximately 11 km in length, is a hilly area located approximately 48 to 59 km from the estuary. A total of 16 lateral structures and 11 levees/bank revetments (Table 1; the locations are presented in Figures 1C and 5F) have been constructed within this study reach. The lateral structures include two weirs (locations 2 and 7 in Figure 1C), six bridges (locations 1, 3, 5, 6, 10, and 16 in Figure 1C), and eight drop structures (locations 4, 8 to 9, and 11 to 15 in Figure 1C). The Renyitan Reservoir (location 17 in Figure 1C) is an off-stream reservoir that intakes water from the Renyitan Weir (location 7 in Figure 1C).

The geological conditions of the study reach are presented in Fig. 2. The Chukou Fault is a high-angle thrust fault that dips eastwards with a stratigraphic throw that exceeds 2000 m. Topographically, the fault separates the Alishan Mountain Range and the Western Foothills, and geologically, the fault is the strata boundary between the Pliocene and Pleistocene epochs. The study reach is located west of the Chukou Fault. The strata orientation dips 10 to 30° westward and is affected by the upthrow of the Chukou Fault. The Bachang River flows toward the west and develops a typical dip stream within the study reach. The bedrock is composed of sedimentary rocks from the Pleistocene and includes the Liuchungchi (Lc) Formation, Kanhsialiao (Kh) Formation, Erhchungchi (Ec) Formation, and Liushuang (Ls) Formation. Lithologically, the bedrocks are chiefly composed of shale, sandy shale, and mudstone, and fine- to medium-grained thick sandstone is interlaid between the major rocks with occasional thin interlayers of sandstone and shale. The unconfined compressive strength of the bank rocks is generally less than 10 MPa and is estimated from Schmidt hammer tests (using a SilverSchmidt type BN hammer with a mushroom plunger) conducted during field investigations. The bedrock strength might be less than the bank rock because of an increase in moisture content (Chang et al., 1996).

Landscape changes could be significantly influenced by tectonics (Schumm, 1979). The Chukou Fault is a significantly active fault in southwestern Taiwan, and GPS survey data demonstrate that the crustal strain near the Chukou Fault was uniform but did not have a detectable vertical deformation (Yu and Chen, 1998; Hung et al., 1999). The average uplift rate of 5 to 7 mm/year in the Central Range is considerably high compared to worldwide rates (Li, 1976; Liu, 1982). As a result, the average local river incision rate is also high and may reach some tens of mm/year in the southern area of the Western Foothills (Dadson et al., 2003). However, the rates are significantly lower than the meter-scale rate within the study reach. Therefore, it is reasonable to infer that regional tectonics are not a predominant factor in the intense channel evolution.

The stream gauging station of Chukou has a drainage area of 83 km^2 and is located in the upstream area of the study reach (Figure 1B). According to the Chukou station records from 1967 to 2011, the annual average daily discharge is approximately 6.5 m^3/s (WRA, 1967 to 2011). The peak flood discharge caused by typhoons is typically less than 1000 m^3/s (Figure 3). The stream flow affected by precipitation demonstrates a significant difference between the wet and dry seasons. During typhoon Herb in 1996, the rain gauge station of Alishan (approximately 25 km north-east of Chukou) recorded rainfall exceeding 80 mm/h for 14 consecutive hours (Wu and Kuo, 1999). The

Table 1
The major events with respect to the study reach.

Year	Major events of human activity/floods with peak discharge >1000 m^3/s	Structure no.[a]/peak discharge
1940s	Construction of the old Wuhuliao Bridge; destroyed in 1988 flood	Not shown in Fig. 1C (2012 image)[b]
1967	Typhoon Clara	1450 m^3/s
1970s	Construction of the Wufeng Bridge; bridge abutment was destroyed in typhoon Morakot of 2009 and repaired that same year	No. 6 in Fig. 1C
1979	Construction of the Renyitan diversion levee	Label d in Fig. 5F
1980	Construction of the Wuhuliao Bridge; destroyed in typhoon Sinlaku of 2008 and reconstructed in 2009	No. 3 in Fig. 1C
1980 to 1987	Construction of the Renyitan Reservoir	No. 17 in Fig. 1C
1983	Construction of the Renyitan Weir; second still basin built in 1991; third still basin built in 1993; regular maintenance after significant floods	No. 7 in Fig. 1C
1983	Construction of the Hsinfu bank revetment	Label e in Fig. 5F
1984	Construction of the Shihkuaitsuo No. 2 bank revetment	Label b in Fig. 5F
1984	Construction of the Chungyi levee	Label k in Fig. 5F
1985	Construction of the Jinlan levee	Label i in Fig. 5F
1985	Construction of the Renyi levee	Label g in Fig. 5F
1987	Construction of the Neiwong levee	Label h in Fig. 5F
1988	Construction of the Shihkuaitsuo No. 1 bank revetment	Label c in Fig. 5F
1989	Typhoon Sarah	1200 m^3/s
1989	Construction of the Chushan levee	Label f in Fig. 5F
1990	Typhoon Yancy	2510 m^3/s
1991	Construction of drop structure downstream from the Wuhuliao Bridge; repaired in 1997, 1999; destroyed by typhoon Sinlaku in 2008; repaired in 2008 and destroyed in 2009	No. 4 in Fig. 1C and details in Fig. 6
1991	Construction of the Nioupu bank revetment	Label a in Fig. 5F
1993 to 1994	Construction of the Fushow levee	Label j in Fig. 5F
1996	Typhoon Herb	2866 m^3/s
1996	Construction of drop structure downstream of the Renyitan Weir; repaired in 2002, 2006, 2008, and 2009	No. 8 in Fig. 1C
1998	Construction of the Hsingyuan Bridge	No. 1 in Fig. 1C
1999	Construction of the Chukou Weir; repaired in 2007, 2008, 2009, 2010, and 2011	No. 2 in Fig. 1C
1999	Construction of drop structure downstream of the Renyitan Weir; destroyed in 2001; repaired in 2006	No. 9 in Fig. 1C
1999	Construction of the Renyitan Bridge[c]	No. 10 in Fig. 1C
1999	Construction of series drop structures; repaired in 2003	Nos. 11 to 15 in Fig. 1C
2001	Construction of the Freeway Bridge	No. 16 in Fig. 1C
2006	Heavy rain	1902 m^3/s
2007	Typhoon Krosa	1276 m^3/s
2008	Typhoon Sinlaku[d]	524 m^3/s
2009	Typhoon Morakot	1010 m^3/s
2010	Construction of the new Wuhuliao Bridge	No. 5 in Fig. 1C

[a] Number of lateral structures (1 to 17) denoted in Fig. 1C; letter of levees (a to k) denoted in Fig. 5F.
[b] The location of the old Wuhuliao Bridge is presented in Fig. 5B (downstream of No. 3) and detailed in Fig. 6.
[c] The old name of the Renyitan Bridge was the Hsinshang Bridge, which was a small bridge (Figure 7A) constructed before 1981. The Hsinshang Bridge was destroyed in the 1988 flood and rebuilt in 1990; it was then destroyed again in the 1996 typhoon Herb. The name was changed to the Renyitan Bridge after it was rebuilt in 1999.
[d] Typhoon Sinlaku is listed because the Wuhuliao Bridge was destroyed during this typhoon period.

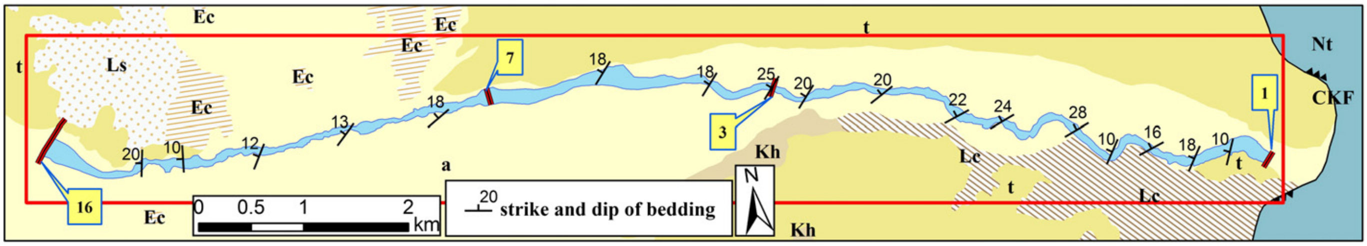

Fig. 2. The geological map of the study reach. Abbreviations of the strata names are listed from older to younger. In the Pliocene epoch: Nt, Niaotsui Formation. In the Pleistocene epoch: Lc, Liuchungchi Formation; Kh, Kanhsialiao Formation; Ec, Erhchungchi Formation; and Ls, Liushuang Formation. In the Holocene epoch: t, terrace deposit; and a, alluvium. CKF: Chukou Fault. The red thick lines denote the locations of lateral structures described in Fig. 1. The red rectangle denotes the location in Fig. 1.

instantaneous peak discharge exceeded 2500 m^3/s in the Chukou gauging station during typhoon Herb and corresponds to the flood discharge from an approximately 200-year return period. The estimated flood discharge of Chukou that corresponds to 2-year and 10-year flood discharges are 389 and 841 m^3/s, respectively (WRA, 2011). The flood events with a peak discharge that exceed 1000 m^3/s are listed in Table 1 for reference.

Digital photogrammetric techniques can be applied to a systematic collection of historical aerial photographs (Lane, 2000; Schiefer and Gilbert, 2007) so that aerial photographs can be extensively used for landscape studies (e.g., Dewitte et al., 2008; Huang et al., 2013b). The topographic data used in this study (Table 2) included one set of topographic maps and six sets of aerial photographs for the past 100 years. A multistage digital surface model (DSM) and aerial orthophotograph were derived from the aerial photographs using a commercial program with a set of ground control points (GCP). The GCPs were derived from the historical 1/5000 photo base maps. The three sets (1981, 1991, and 1999) of aerial photographs, which had a nominal ground pixel size of 0.2–0.3 m, were purchased from the Aerial Survey Office of the Forestry Bureau of Taiwan, which periodically collected aerial photography for land resource surveys since the 1970s. Camera calibration reports were available for these historical aerial photographs, and the reports provided detailed geometric parameters of the camera systems to improve model accuracies. The mean and standard deviation of the GCP residuals are provided in Table 2. Because the aerial photos indicated sparse vegetation in the channels, the DSMs were applied without further editing. The topographic data for 2004 and 2009 were collected from the project results of the Water Resources Agency, and the data accuracies were verified under the requirements of the projects. The cross section survey data (Table 2) were used to analyze the channel-change trend of the DSMs because the cross sections of 500 to 1000 meter intervals were not sufficient to describe the terrain changes. The datum system of the 1904 topographic map was different from the other topographic data; nevertheless, the landform characteristics of the 1904 topographic map were comparable to the 1981 topographic data. Hence, the contours of the 1904 topographic map were adopted as a reference to reveal the relative terrain changes.

3. The changes of river morphology

Human activity has significantly changed the channel morphology of the study reach. Over several decades, armoring materials have gradually disappeared and caused the underlying bedrock to suffer severe erosion. The channel morphology has transformed to a steep valley with a maximum incision depth of 30 m (Figure 4). The three main types of human impact in this reach are lateral structures, sediment mining, and stream-bank protection structures. Based on the chronological topography data, the channel changes in planform, longitudinal profile, channel width, and cross sections are described with schematic illustrations.

3.1. The changes in channel planform

The channel planforms were delineated from the aerial orthophotos to illustrate the channel migrations (Figure 5). The outline of the channel planform was approximate to the area of the bankfull channel

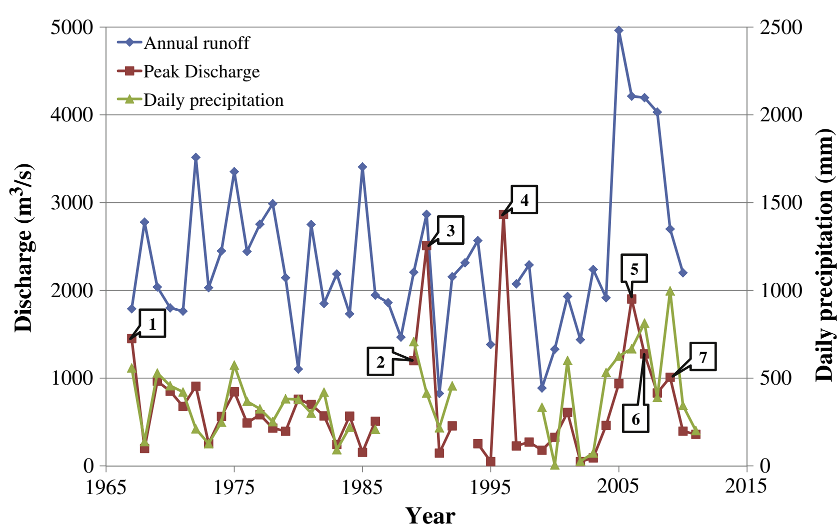

Fig. 3. The discharge and precipitation data of the Chukou station from 1967 to 2011 (WRA, 1967 to 2011). The annual runoff is the summation of the average daily discharge. The peak discharge is the instantaneous peak discharge. The daily precipitation is the precipitation on the date of the peak discharge. The rectangle numbers denote the major flood events listed in Table 1. Broken lines indicate no data available.

Table 2
Summary of the topographic data.

Year	Data type [a]	GCP residuals [b]	Data resolution
1904	1/20,000 topographic map	–	Contour intervals 25 shaku (plains) and 50 shaku (hills) [c]
1981	Photogrammetry (11 BW photos)	0.07 (1.99) m	1 m
1989	Cross section survey	–	Section interval at approximately 500 m
1991	Photogrammetry (16 BW photos)	0.07 (1.91) m	1 m
1996	Cross section survey	–	Section interval at approximately 500 m
1999	Photogrammetry (14 BW photos)	2.34 (3.85) m	1 m
2000	Cross section survey	–	Section interval at approximately 500 m
2004	Photogrammetry (WRA project)	<1 m	5 m
2006	Cross section survey	–	Section interval at approximately 300 m
2008	Cross section survey	–	Section interval at approximately 300 m
2009	Photogrammetry (WRA project)	<1 m	5 m
2012	Airborne LiDAR	<1 m	1.5 pts/m^2

[a] BW indicates panchromatic photography; the data for 2004 and 2009 are collected from the project results of the Water Resources Agency.
[b] Ground control point (GCP) residuals: mean (standard deviation); the required DEM accuracy of the WRA projects are less than 1 m.
[c] Shaku = 10/33 m, traditional measurement units of Japan.

determined by the aerial orthophotos with the exception of the outline of the channels in 1904, which was obtained from the topographic map. The bankfull channel indicates the area that is associated with frequent discharge and includes low-flow channels, areas of sparse vegetation cover and recently deposited sediments (Rosgen, 1996).

In 1904, the channel type was a single-thread meandering type in the upstream region, and it changed to a bar-braided type in the downstream region (Figure 5A). No artificial structures were found on the 1904 topographic map.

In 1981, the channel planform was similar to the geometry of 1904 with the exception of instream gravel mining within the reach beginning in the late 1970s. Three bridges had been built (Table 1) across the river: the Wuhuliao Bridge (Figure 5B, No. 3), old Wuhuliao Bridge (destroyed in a 1988 flood; Figure 6B), and Wufeng Bridge (Figure 5B, No. 6). Moreover, a diversion levee (label d in Figure 5F) was constructed upstream of the Wufeng Bridge for water extraction from the Renyitan Weir (completed in 1983; Figure 5C, No. 7) to the Renyiran Reservoir (completed in 1987; Figure 1C, No. 17). The levee has shrunk the channel width to approximately one third of its original width.

In 1991, instream gravel mining remained significantly active throughout the reach. A total of nine levees (labels a, b, c, e, f, g, h, i, and k in Figure 5F) were constructed within this reach, six of which were located in the downstream area of the Renyitan Weir. After the old Wuhuliao Bridge was destroyed in a 1988 flood (Figure 6), drop structures (Figure 5C No. 4) were installed to protect the Wuhuliao Bridge. The channel width had narrowed compared to the channel width in 1981. There were two braided channels that were located approximately 1 km downstream from the Renyitan Weir (Figure 7). The northern-channel was the main channel during this period.

For the period from 1991 to 1999, the channel was continuously incised and narrowing as a result of human impact and large floods. Additional structures were constructed in the channel to protect the existing infrastructure (Figures 6 and 7). The drop structures were constructed downstream of the Wuhuliao Bridge following the 1988 floods, and they included a check dam and stilling basin (Figure 6B). The subsequent maintenance and extension rendered drop structures that consisted of three check dams and still basins (Figure 6C).

The Renyitan Weir (Figure 5C No. 7) was completed in 1983, and it is the most important structure in the study reach. There was a consistent issue with scour since the weir's construction (Figure 4C and D), and a series of engineering countermeasures (Figure 4E) were conducted that included an 1) extension of two stilling basins and side wall protection; 2) riprap of concrete blocks with concrete cement; 3) secondary dam with a pile foundation; 4) concrete pavement; and 5) two drop structures downstream of the weir (Figure 5D, Nos. 8 and 9). All of the countermeasures have been constantly repaired following typhoon floods to ensure the safety of the Renyitan Weir.

In 1999, gravel mining almost ended in this reach for two reasons: first, only a thin layer of sediment remained above the exposed bedrock as shown in the aerial photos; second, gravel mining was banned because of increasing channel incision. The most significant change in this period was the flow diversion from the northern channel to the southern channel approximately 1 km downstream of the Renyitan Weir (Figure 7). The southern channel was deeply incised following typhoon Herb in 1996. Consequently, the bed elevation of the southern-channel was lowered compared to the northern channel, which had previously represented the main channel (Figure 7A). The northern channel was gradually abandoned and then enclosed by the levee that was built along the southern channel (Figure 7B). In addition, the severely incised southern channel caused the failure of the Renyitan Bridge (Figure 5D, No. 10; originally a small bridge named the Hsinshang Bridge) during typhoon Herb, and the Renyitan Bridge was rebuilt in 1999. Many lateral structures were constructed for grade control (Figure 5D, Nos. 8 to 9 and 11 to 15). Two structures, the Singyuan Bridge (Figure 5D, No. 1) and Chukou Weir (Figure 5D, No. 2), were constructed in the upstream area of the reach.

In the periods from 1999 to 2004, 2004 to 2009, and 2009 to 2012, the channel planforms were relatively stable. The Freeway Bridge (Figure 5E, No. 16) in the downstream area was completed in 2001. The Wuhuliao Bridge was destroyed in typhoon Sinlaku of 2008 (Figure 4B) and reconstructed in 2009 (Figure 6D), and the Wufeng Bridge was destroyed during typhoon Morakot of 2009 and reconstructed the same year. Moreover, the new Wuhuliao Bridge (Figure 5F No. 5) was also constructed approximately 500 m downstream from the Wuhuliao Bridge as a replacement. Although other lateral structures remained unchanged, various maintenance and repairs were conducted after each severe flooding incident, especially on the two weirs.

3.2. The changes in longitudinal profile

The chronological longitudinal profiles (Figure 8) were drawn based on the stream thalweg taken from the topographic data (Table 2). The location and maximum incision depth for each period are denoted in Fig. 8. The longitudinal profile for 2004 can be divided into five sub-reaches by using four artificial knickpoints (Figure 8E): the drop structure No. 3 (DS3), Renyitan Weir (RYTW), Wuhuliao Bridge (WHLB), and Chukou Weir (CKW), in which the man-made structures fix the local base level. Sub-reach 1 (SR1) is the downstream sub-reach of DS3, sub-reach 2 (SR2) is located between DS3 and RYTW, sub-reach 3 (SR3) is located between RYTW and WHLB, sub-reach 4 (SR4) is located between WHLB and CKW, and sub-reach 5 (SR5) is upstream at CKW. These five sub-reaches were adopted for the following discussion and analysis.

Fig. 8A presents the longitudinal profiles for 1904 and 1981. The longitudinal profile for 1904 was obtained from the contours of the 1904

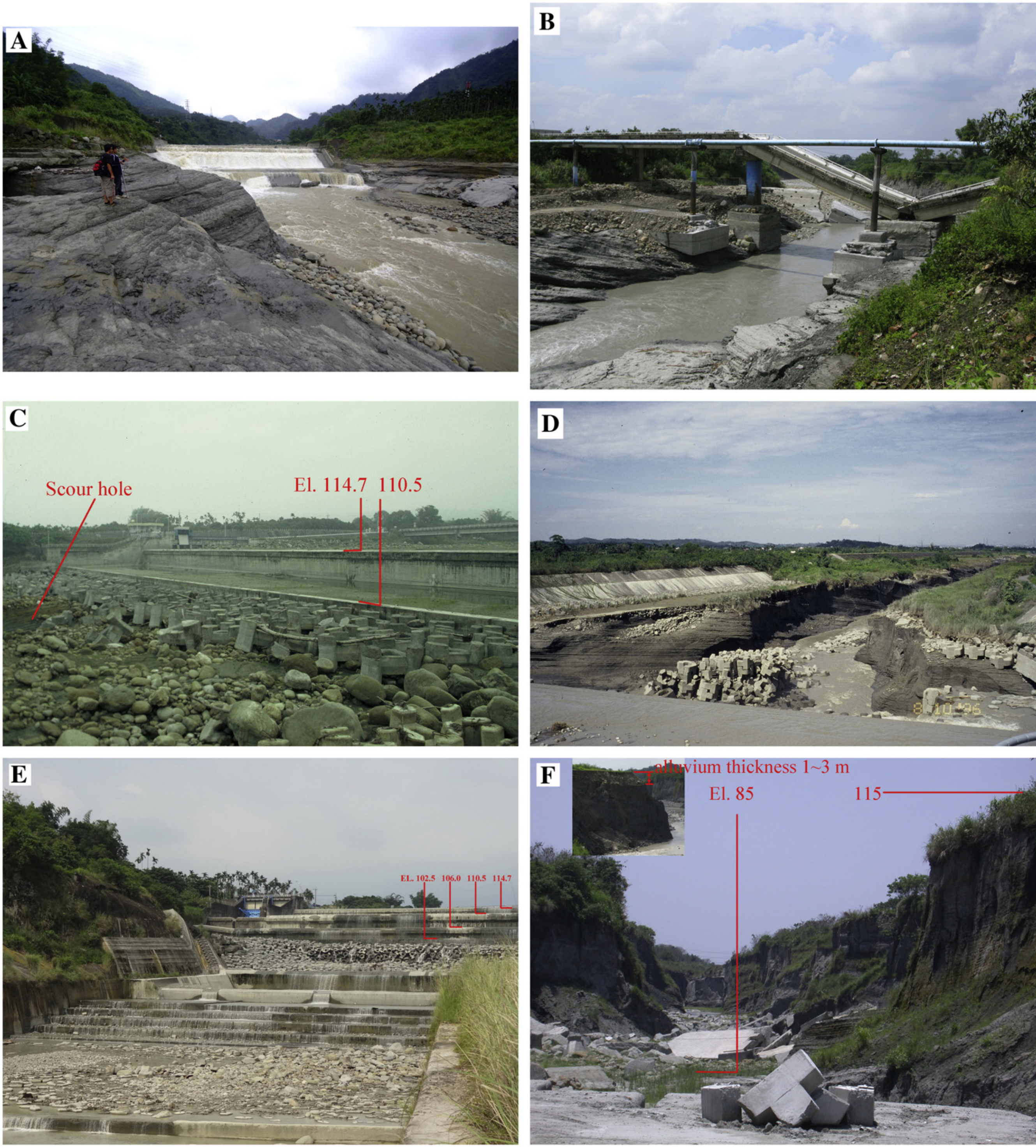

Fig. 4. The channel morphology has significantly changed as a result of human intervention. (A) Local scour downstream from the Chukou Weir (sub-reach 4) caused the weak mudstone to be exposed and deeply incised. (B) The Wuhuliao Bridge (view from upstream; sub-reach 4) was destroyed as a consequence of drop structure failure from typhoon Sinlaku of 2008. The knickpoint of the drop structure has retreated rapidly and formed a deep narrow channel. (C) The Renyitan Weir was designed as a low-head dam with a stilling basin (sub-reach 2). The problem of local scour occurred following the weir construction (courtesy of WRA, Taiwan). (D) The deeply incised bedrock channel downstream of the Renyitan Weir (sub-reach 2) occurred following typhoon Herb of 1996 (courtesy of WRA, Taiwan). (E) A series of engineering countermeasures (sub-reach 2) were conducted to protect the Renyitan Weir . (F) A narrow and steep-sided valley (view from upstream) is now the typical channel morphology in the study reach. The height of steep rock bank could be up to 30 m downstream of the Renyitan Weir. The upper-left small photo shows the alluvial deposition on the rock bank (sub-reach 2).

map with limited resolution and different control points. However, the two longitudinal profiles appeared similar with minor variations. Several sections of the 1981 profile could have been affected by the gravel mining since the late 1970s; however, the effects are not yet obvious. Both profiles were similar to a straight line compared to the profiles in the later years. The entire reach attained a smooth slope in dynamic equilibrium. The profile (prior to 1981) was likely the result of natural balance with insignificant anthropogenic influences. When a graded stream is subject to disturbances from either natural or human factors, it adjusts itself to re-establish the equilibrium profile

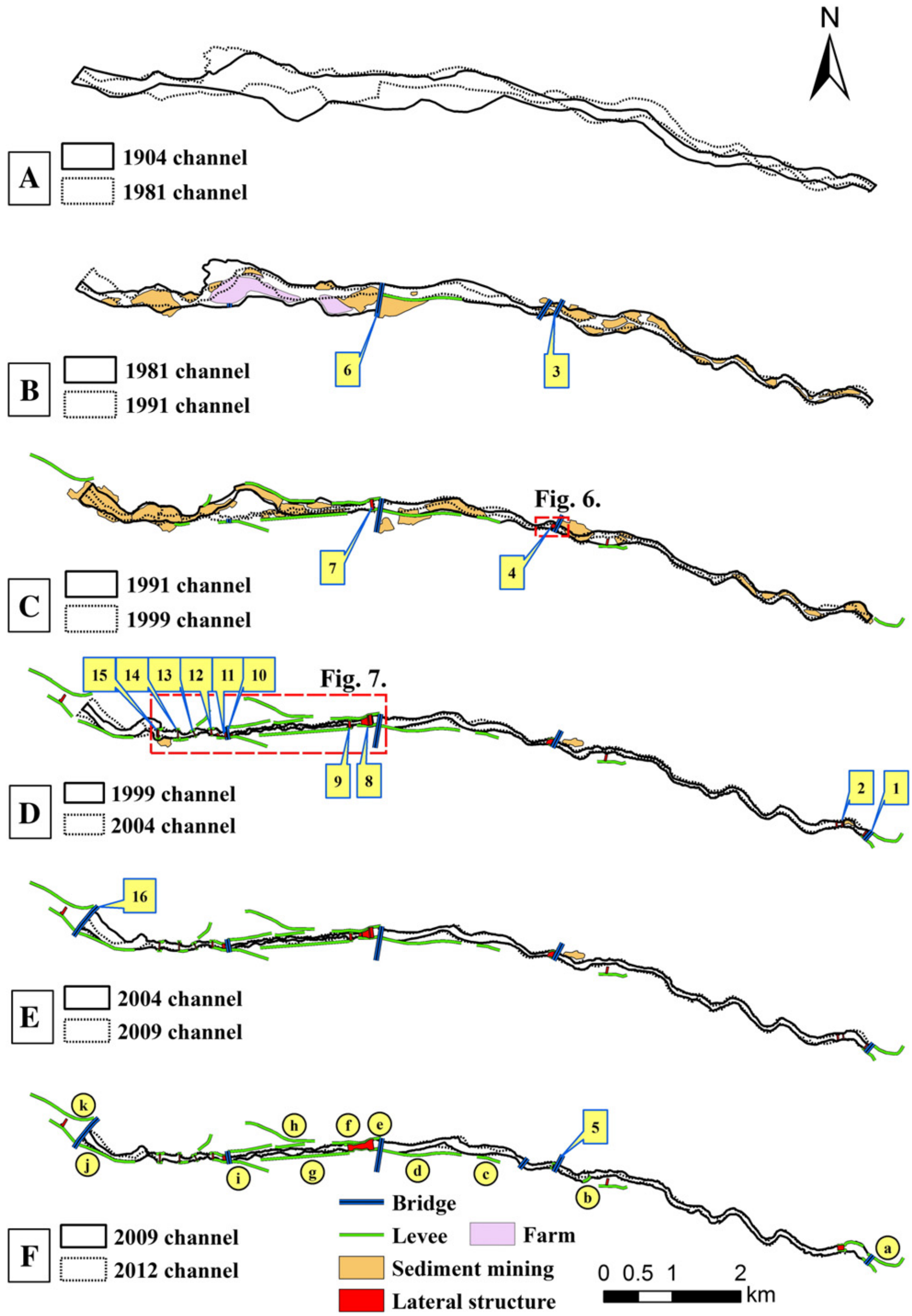

Fig. 5. The changes in the channel planform for each period. (A) 1904; (B) 1981; (C) 1991; (D) 1999; (E) 2004; and (F) 2009. The structure numbers that are identical in Fig. 1 denote only the year following the structure completion. The red dash rectangles are the areas presented in Figs. 6 and 7. The major events related to the lateral structures and levees are listed in Table 2.

(Lane, 1955). The new equilibrium profile is then preserved as long as the factor(s) exists. With respect to the Bachang River, the natural influence is insignificant relative to the effects of human disturbance.

General channel degradation was demonstrated in the longitudinal profile from 1981 to 1991 (Figure 8B) with the exception of two areas: the Renyitan Weir and Wuhuliao Bridge. The general degradation of the channel was caused by extensive gravel extraction along the river. The local scour of the Renyitan Weir occurred on the downstream side, and sediment was deposited in the upstream side. The bed elevation of the Wuhuliao Bridge was controlled by the drop structure built following the 1988 flood. Two artificial knickpoints were gradually formed in RYTW and WHLB because the structure fixed the bed elevation. Other knickpoints may be formed in the upstream boundary of the gravel pit (Kondolf, 1994). The retreat of a gravel pit knickpoint could be found at an approximate distance of 1500 m, which is shown in Fig. 8B. The maximum depth of the channel incision was 12.9 m and located at a distance of 900 m, which is shown in Fig. 8B.

From 1991 to 1999 (Figure 8C), the channel incision occurred mainly in the downstream area of the RYTW and upstream area of the WHLB. Gravel mining was the main cause of bed degradation in the upstream area of the WHLB. In the downstream area of the RYTW, the channel incision was caused by the two processes: the knickpoint migration of the

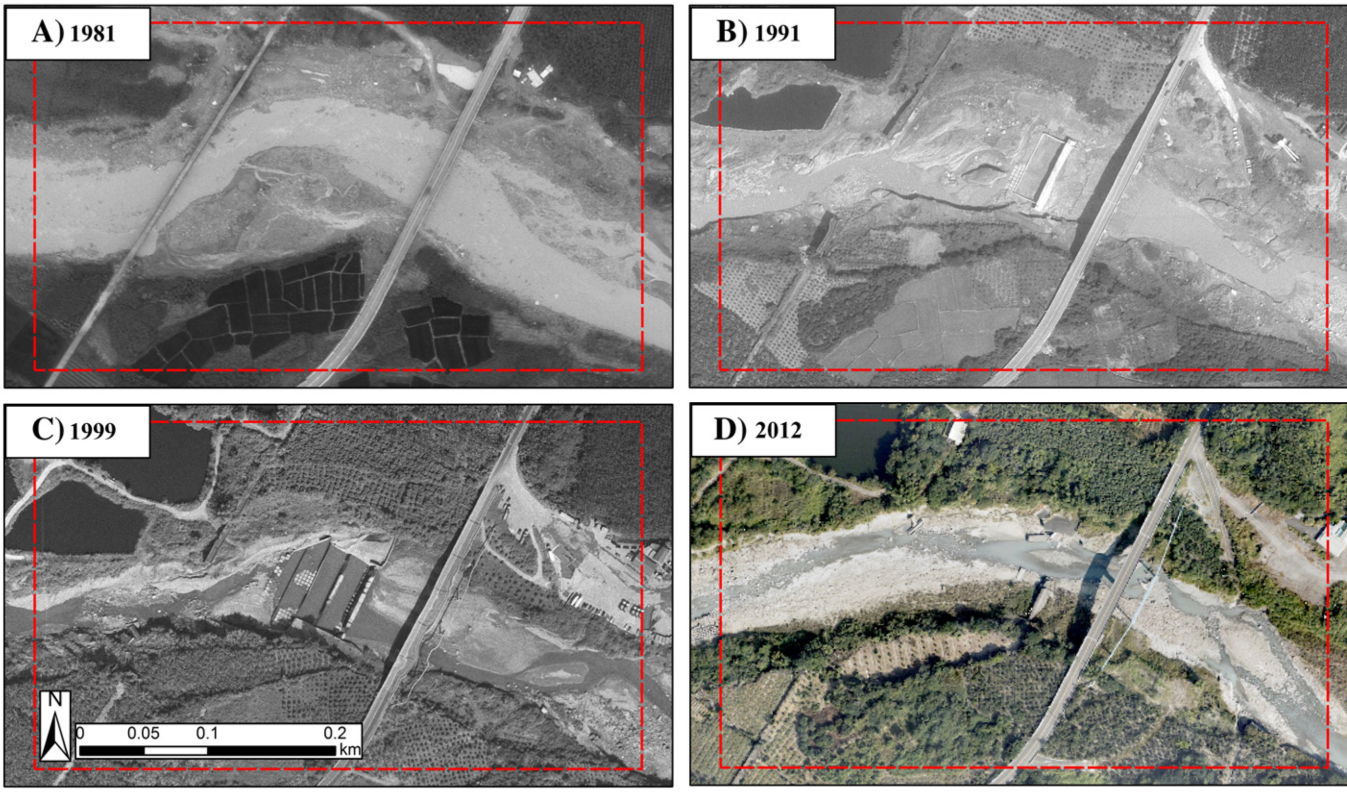

Fig. 6. The changes in channel planform in the vicinity of the Wuhuliao Bridge. (A) 1981: old Wuhuliao Bridge (left) and Wuhuliao Bridge (right); (B) 1991: the old Wuhuliao Bridge was destroyed by a flood in 1988. The drop structure was constructed on the downstream side of the Wuhuliao Bridge; (C) 1999: a series of drop structures were constructed to protect the Wuhuliao Bridge; (D) 2012: the Wuhuliao Bridge was destroyed during typhoon Sinlaku of 2008 and reconstructed in 2009. The location of the red dash rectangle is presented in Fig. 5B.

gravel pit and extension of local scour toward the downstream direction. Consequentially, the incision rate was rapid and the accumulated incision depth approached 30 m because of the combined effects of the two erosion processes since 1981. The local scour of the WHLB was limited in the downstream side because the base level was fixed by the RYTW. The Chukou Weir was completed in 1999 and formed another knickpoint. The maximum depth of the channel incision was 17.2 m and located at a distance of 2755 m.

A series of drop structures were constructed as countermeasures to resolve the problem of channel degradation and improve the stability of the existing infrastructure. From 1999 to 2004 (Figure 8D), the channel incision was limited in the downstream side of the RYTW and WHLB. The furthermost downstream drop structure, DS3, formed a new knickpoint. The maximum depth of the channel incision was 8.1 m and located at a distance of 3890 m.

From 2004 to 2009 (Figure 8E), the local scouring process was active downstream of the CKW (Figure 4A). The maximum depth of the channel incision was 6.3 m and located at a distance of 10,875 m. Because the drop structure at WHLB was destroyed by typhoon Sinlaku in 2008, the WHLB knickpoint (approximately 15 m in height) was no longer fixed by the structure. The WHLB knickpoint rapidly migrated upstream and sediments were transported to and deposited in the downstream area of the knickpoint.

The main change between 2009 and 2012 (Figure 8F) was caused by the restoration process in the WHLB sub-reach area. The longitudinal profile was gradually restored to a smooth gradient. The maximum depth of the channel incision was 6.0 m and located at a distance of 6820 m. Although the local scour downstream of the CKW remained active, the channel downstream of the CKW was slightly aggraded during this period. The cause of the channel aggradation was a large quantity of sediment brought by typhoon Morakot in 2009 and deposited in the CKW sub-reach.

The features of the five sub-reaches, including the average channel incision, average channel width, and cross section, are discussed in the following sections.

3.3. The changes in average channel incision

With the exception of the maximum incision depth for each period presented in Fig. 8, the average depth of channel incision was calculated to reflect the average graded condition in each sub-reach for each period (Figure 9A). The maximum average incision depth was 8.7 m in sub-reach 1 for the period from 1981 to 1991. Because sediment was mined from the downstream to upstream, the channel erosion downstream was greater than the channel erosion upstream.

During the period from 1991 to 1999, sub-reach 2 possessed the maximum average incision depth of over 10 m because of the erosion processes from the pit knickpoint migration and downstream extension of the RYTW local scour. Sediment mining gradually moved upstream and enlarged the magnitude of the channel erosion in sub-reach 4. The incision depth was smaller in sub-reaches 1 and 3 compared to sub-reaches 2 and 4.

In the periods from 1999 to 2004, 2004 to 2009, and 2009 to 2012, with the exception of the exacerbated local scour of the CKW, the average incision depths gradually decreased and even became aggraded in sub-reaches 1 and 3. In sub-reach 5, the channel condition was directly affected by the sediment yield from the mountain basin. The channel of sub-reach 5 was in a mostly aggraded condition with the exception of the period from 1991 to 1999 when the channel was also deeply mined.

3.4. The changes in average channel width

The channel width may reflect an adjustment of the channel morphology. In this study, the channel width was estimated from the

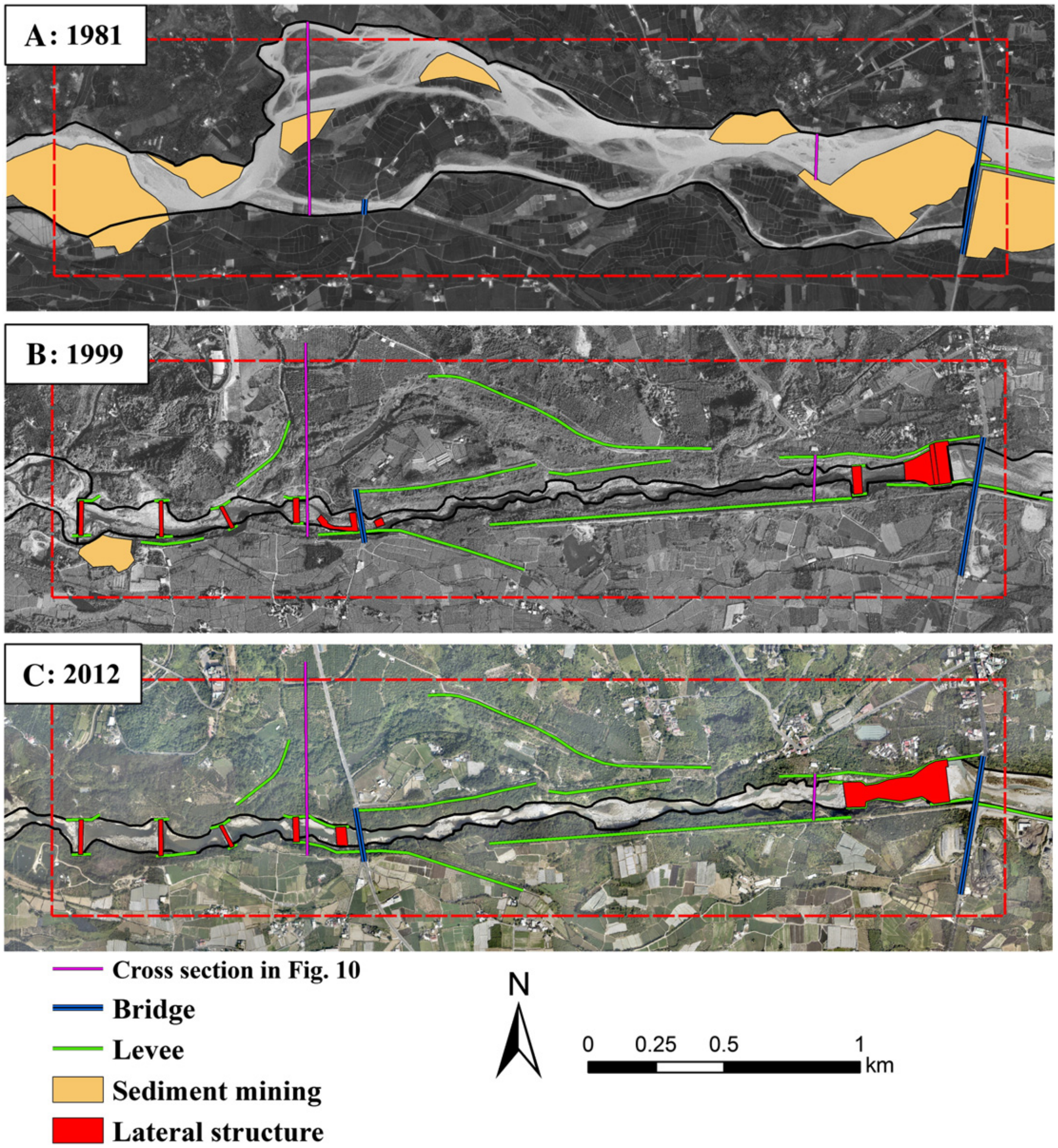

Fig. 7. The changes in channel planform downstream of the Renyitan Weir. (A) 1981; (B) 1999; (C) 2012. The location of the red dash rectangle is presented in Fig. 5C.

channel area and channel length. The areas of each sub-reach (except for the areas of farm land) were calculated from the channel planforms (Figure 5). The channel lengths of the sub-reach were measured along the channel centerline from the aerial orthophotos. The average channel width was defined as the channel area divided by the channel length. Fig. 9B presents the chronological data of the average channel width.

The average channel width of sub-reaches 2 to 4 decreased rapidly before 1999 and exhibited small range variations afterwards. The average channel width of sub-reach 1 also demonstrated a declining trend but with a substantial variation. The data for sub-reach 5 were varied in a range without a trend. The maximum width change decreased from 448 m to 73 m in sub-reach 2 because the channel pattern had changed from a double-thread braided type to a single-thread valley type. The ratio of the channel-width change for the other sub-reaches was between 2.1 and 3.4 with the exception of sub-reach 5 (no change in width). The trend of channel width change was compatible with the degree of channel incision; more incised channels such as sub-reaches 2 and 3 possessed a larger change ratio in channel width (Figure 9). Additionally, the features of channel-width change in response to the incision were distinct between the alluvial channels and bedrock channels: the width of the bedrock channels (sub-reaches 2, 3, and 4) changed in a stable trend, whereas the alluvial channels (sub-reaches 1 and 5) with easily erodible banks demonstrated a variable trend. However, most of the channels were gradually confined to the deep-incised valleys or the artificial levees with limited dimensions for channel variation.

3.5. The changes in the channel cross sections

Changes in the channel cross sections could also reflect a channel transformation in addition to being an indicator of the channel planform. Two cross sections are presented in Fig. 10. The two cross sections belong to sub-reach 2, which were originally composed of a multi-thread and single-thread channel. Cross section A was located approximately 1 km downstream from the RYTW (Figure 7A) and demonstrated that the channel had shrunk considerably as a result of the levee construction prior to 1991 (Figure 5C). The channel of cross section A was deeply incised with steep rock banks (e.g., Figure 4F) with an average rate of 1.3 m annually from 1981 to 2004. After this period, the

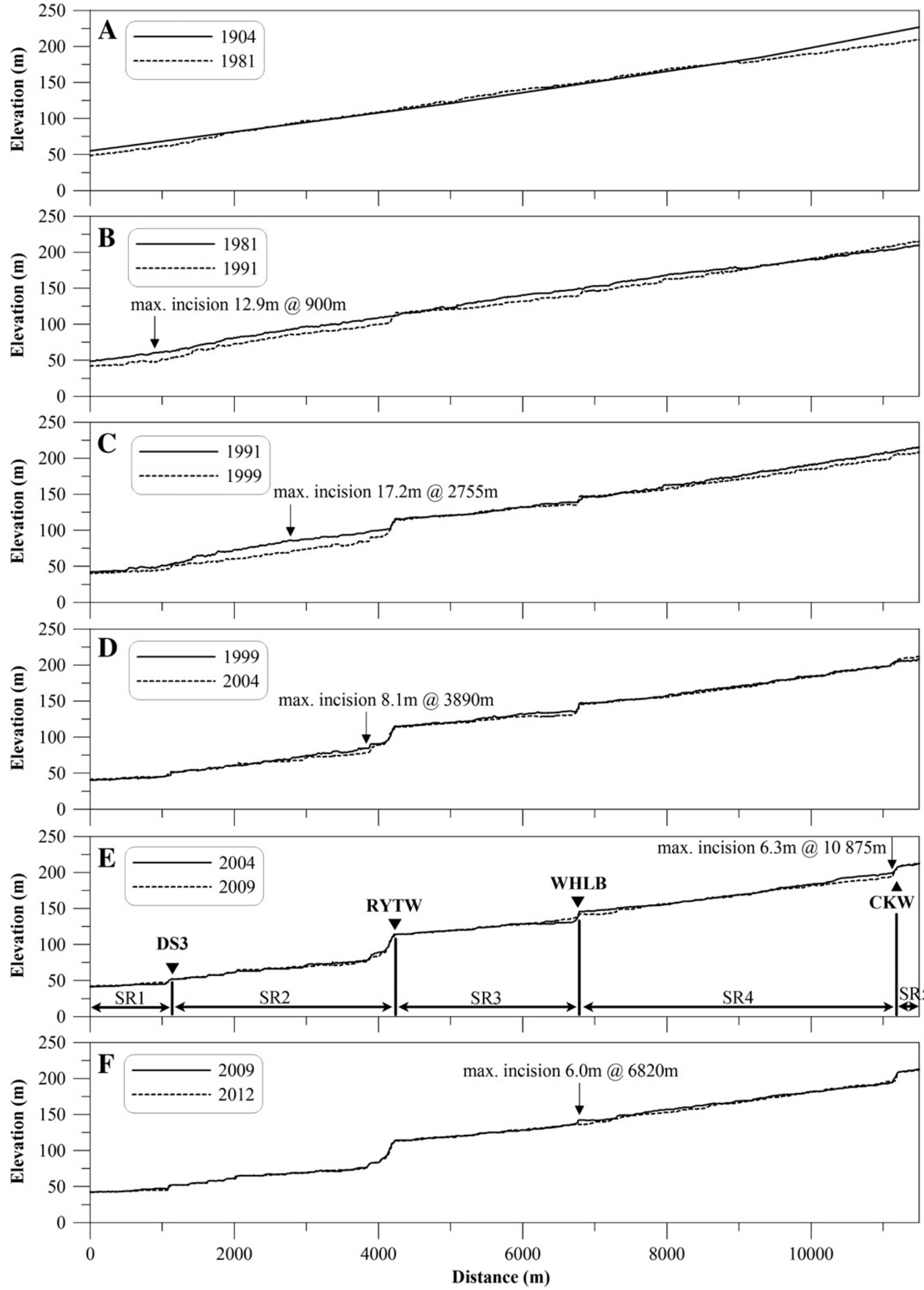

Fig. 8. A comparison of the longitudinal profile for each period. The abbreviations in subpanel E stand for the following structures. DS3: Drop Structure No. 3; RYTW: Renyitan Weir; WHLB: Wuhuliao Bridge; CKW: Chukou Weir; SR: sub-reach.

channel widening became the main erosion process. The channel type for cross section B was originally braided with a multi-thread channel (Figure 7A). The stream flow was diverted from a northern to southern channel in 1996 because the southern channel was deeply incised during typhoon Herb. The profiles of cross section B (Figure 10B) demonstrated the deeper channels in 1991 that were located at a distance of approximately 300 m and then shifted to a distance of approximately 100 m in 1999. The channel area was significantly reduced and narrowed.

3.6. The changes in flow velocity and stream power

The flow velocity and stream power could also change because of significant changes in the channel geometry. According to the WRA

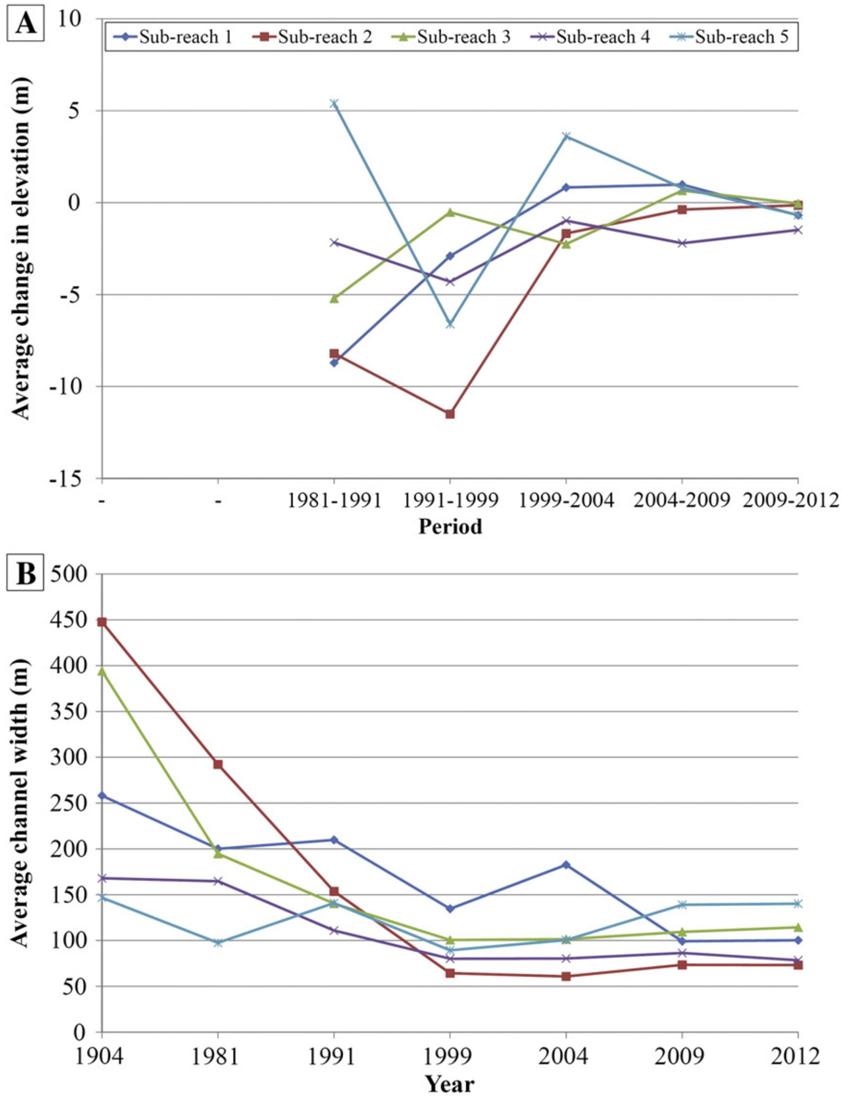

Fig. 9. (A) The changes in the average channel incision in each sub-reach; (B) The changes in the average channel width in each sub-reach.

reports of the Bachang River (WRA, 1990, 2006), the average flow velocities in the cross-sections A and B for a discharge of 1040 m^3/s and the 1989 cross-section data were 4.2 and 3.0 m/s (Figure 10), respectively, and for a discharge of 1200 m^3/s and the 2006 cross-section data, were 9.2 and 7.6 m/s, respectively. With a 15% difference in discharge, the magnitude of the average flow velocity increased more than twice

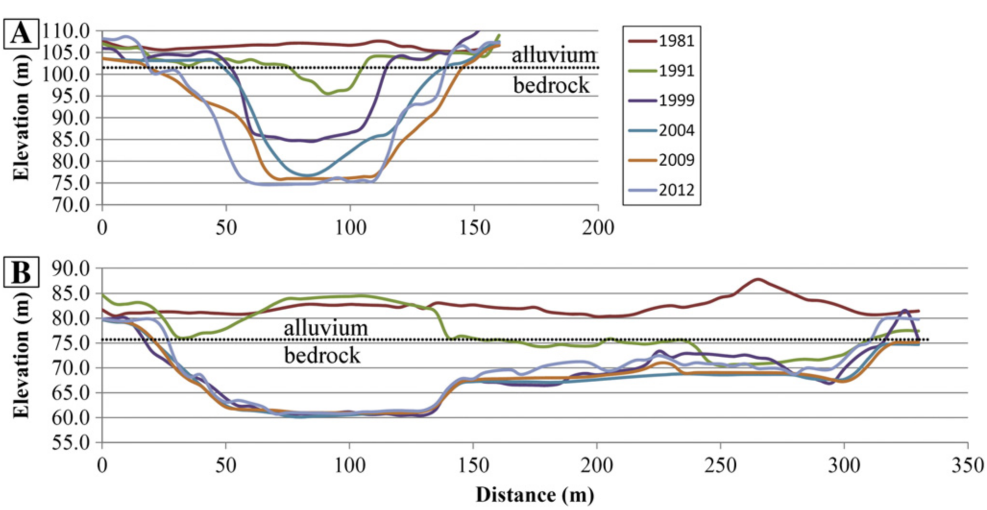

Fig. 10. The change in the typical cross sections. The locations of the cross sections are indicated in Fig. 7. The dotted lines denote the possible boundary of alluvium and bedrock.

from 1989 to 2006 because of the change in channel geometry. With the hydraulic data of the Bachang River (WRA, 1990, 2006), we further calculated the stream power in the cross sections A and B (which was equal to the shear stress multiplied by the flow velocity). The stream powers in 1989 in the cross-sections A and B were 868 and 337 W/m^2 (Figure 10), respectively, and in 2006 were 10,265 and 3417 W/m^2, respectively. The magnitude of the stream power increased by an order from 1989 to 2006.

4. The influencing factors on the changes of channel morphology

We inferred that the causes of the channel changes included six factors from two categories: the natural factors, including the geological conditions, bedrock erosion processes, and hydrological conditions; and the human factors, including gravel mining, lateral structures, and levee construction.

4.1. The natural factors

In addition to human factors, natural conditions of the reach are key factors to the channel evolution. The Pleistocene sedimentary rocks in the study reach are soft rocks that are mainly composed of shale, sandy shale, and mudstone with an unconfined compressive strength of less than 10 MPa. All of the soft rock is less durable because of a high clay mineral content and poor cementation (Lee et al., 1996). Once the soft rocks are exposed on the riverbed without an armoring protective layer, the erosion process can rapidly occur (Lai et al., 2011; Huang et al., 2013b).

The orientation of the rock beddings is a dominant factor that influences the erosion process and evolution of a bedrock channel. The study reach is a typical dip channel, and the dip direction of the bedrock is approximately parallel to the flow direction. The rock banks could be self-sustained with a steep inclination after channel degradation. Therefore, the quantity of channel widening is small compared to the evolution of the alluvial channels (e.g., Simon and Rinaldi, 2006). Consequently, the river flow would concentrate in the deep channels and exacerbate channel incision.

The large floods caused by typhoons have significantly enhanced the bedrock erosion process. The average daily discharge of the study reach is 6.5 m^3/s only, whereas the instantaneous peak discharge could be greater than 2500 m^3/s during a typhoon, such as typhoon Herb in 1996 (Figure 3). The difference in the stream discharge can vary significantly, and the significant changes in channel morphology are usually caused by large floods and subsequent structure failure.

4.2. The human factor

The human factors have been the catalyst for the channel evolution in the study reach. A comparison of the channel geometry (such as the channel planform and longitudinal profile) between 1904 and 1981 indicated that the channel morphology had not been significantly changed. The land use of the study reach was low-intensity agriculture during the early period. The demand for sand and gravel for the construction of the Alishan highway in the late 1970s could have signaled the onset of significant human impacts in addition to the large amounts of construction materials required for the Renyitan Reservoir (1980 to 1987), which was mined from the study reach.

The predominant human factors affecting the channel change in the presented case include the following: 1) gravel mining that occurred before 1999; 2) construction of the RYTW in 1983; 3) construction of the WHLB drop structure in 1991; 4) construction of the CKW in 1999; and 5) construction of a series of downstream drop structures at the RYTW in 1999.

Large-scale morphological adjustments were imposed on the river to balance the influence from human disturbance. Instream gravel mining for construction aggregates was considered more economical than alternatives without the environmental cost (Kondolf, 1994). The riverbed elevation and channel profile were directly altered by the gravel extraction (Kondolf, 1997). The sediment storage in the study reach was extensive during the earlier years and a significant source of aggregate. Gravel mining was active during the period from 1981 to 1999; however, there was a lack of data, so an accurate volume of sediment mined from the channels cannot be determined. The bedrock was gradually exposed on the river bed following intense mining, and the riverbed directly suffered from the erosion.

The levee in this reach was first constructed to divert the flow for the RYTW (Figure 5B) and was extended to the downstream area of the RYTW for flood protection. The channel was significantly reduced to one-third of the original river width in certain parts of the reach. The direct impact of the levee was to limit the lateral shift of the river to a narrower and less wandering channel. The flow velocity would increase in a straight and narrow channel and enhance the erosive power of the bedrock.

A lateral structure may produce a change of a river's longitudinal profile in several aspects. Although the Renyitan Weir was just a small dam with a designed height of less than 5 m, the lateral structure severely disturbed the longitudinal profile of the stream because of the scour process of the soft bedrock. The weir resulted in two types of disturbances to the natural equilibrium: first, the sediment was deposited in the upstream side of the weir and could not have been transported downstream; second, the stream power was increased because of an elevated water-level, and it generated a scour hole in the downstream side of the weir. The process of generating scour holes in soft bedrock was not identical to the case of dams built on hard rock (e.g., Bollaert and Schleiss, 2003). A scour hole in soft rock exhibited a low sloping inclination in the upstream side and tended to progress to the downstream (Cheng et al., 2010). The lengthening process of the scour hole might dominate the rapid bedrock incision downstream of the lateral structures.

A lateral structure will also create an artificial knickpoint that sets a boundary condition for the upstream area. With respect to a weir, the local base level is artificially raised and results in aggregation upstream. Within two consecutive lateral structures, the downstream structure will constrain the base level, whereas the upstream structure promotes additional erosion (e.g., sub-reach 3 is between the RYTW and WHLB). Therefore, the average slope is lowered from the original condition. Once a restriction is removed (e.g., destroyed by a flood), the slope readjusts once again and gradually returns to a new equilibrium. The 2008 failure of the WHLB is a good example that demonstrates the post-failure slope readjustment in the sub-reaches 3 and 4 back to a smooth slope (Figure 8E and F).

The lateral structures (e.g., the weirs and grade controls) and longitudinal structures (e.g., the levees) influenced the incision of the river channel in different ways. The levee confined the channel width and impacted the channel incision in the early stages. Once the channel was deeply incised into a gorge-type channel, the confined boundaries were shifted from the levees to the steep rock banks. However, the local scour from the weir did not contribute significantly to the channel incision in the early stages, and it accumulated gradually. As long as the weir persisted, the local scour ahead of the weir would continuously affect the channel condition.

4.3. The interactions of the influence factors

The rapid incision of the river is not possible when using a single factor alone. Each factor contributes an effect to the complex process of morphological adjustment. The natural influence factors are inherent with the graded stream before the channel morphology was changed by human intervention. The morphological changes of rivers discussed in Section 3 demonstrate that human activities altered the conditions of the stream system and activated the function of the natural factors in the erosion processes. The soft bedrock did not immediately suffer from flow erosion, and only began suffering when the armor layer was extensively extracted by the sediment mining (e.g., Figure 7). The erosive capacity of the stream flow was intensified as a result of flow concentration caused by 1) a reduction in channel width because of levee construction in the early years (mostly in the 1980s) and 2) the development of a narrow deep channel in the typical dip stream later. During a large flood, the stream power could be raised more than an order, which is based on the stream power calculation in Section 3.6 and results in a significant decrease of the channel width-to-depth ratio. Lateral structures, such as the weir and drop structures, often caused local scours (e.g., Figures 4 and 8). Furthermore, the artificial knickpoints of the lateral structures might intensify the water erosive power downstream, which is unfavorable to the stability of a narrow-deep channel in this study reach. The backward propagation of the downstream local incision could be enhanced by the natural factors of a dip channel in the soft rock and might further worsen the situation (Figure 4C, D, and E). Occasionally, additional lateral structures were installed in an attempt to control the enhanced incision process (Figures 6, 7, and 8). However, it often turned into a vicious circle (e.g., Figure 6).

5. The channel evolution and lessons learned from the case

5.1. The channel evolution to date

According to the topographic data, the channel evolution of the study reach can be described as in Fig. 11. The key points of the evolution are included below.

Stage 1 demonstrated the onset of large-scale human intervention during the 1980s. Intense gravel mining occurred in many locations and spread the downstream reach in an upstream direction. The RYTW and diversion levee were constructed at this stage.

Gravel mining was intense and widespread in stage 2 of the 1990s. The sediment storage was significantly reduced from years of continuous extraction from excessive mining and the bedrock was gradually exposed in many areas. A scour hole was formed in the downstream RYTW area and extended rapidly in a downstream direction. The knickpoint migration of mining pits was another significant process of bedrock erosion. The bedrock erosion proceeded rapidly and threatened structural stability. The drop structures were constructed for grade

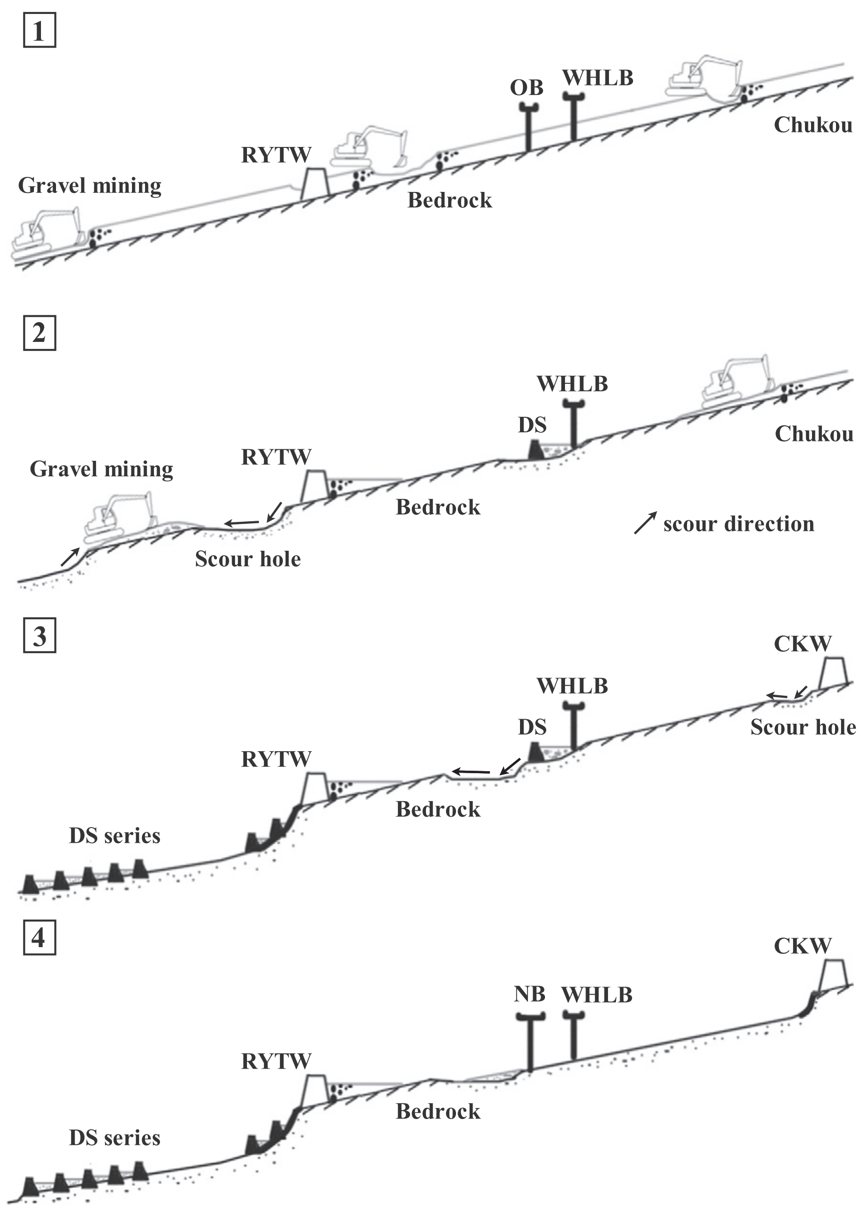

Fig. 11. The stages of channel evolution. RYTW: Renyitan Weir; CKW: Chukou Weir; WHLB: Wuhuliao Bridge; OB: Old WHLB; NB: New WHLB; DS: Drop Structure.

control following the destruction of the old WHLB by the channel incision caused by the typhoon flood.

The channel became narrower and deepened as a result of human alteration in stage 3 during the late 1990s. The rate of channel change was rapid because of the unfavorable natural factors of soft bedrock and significant typhoon flooding. Following typhoon Herb in 1996, a severe incision produced a straight channel in the downstream area of the RYTW. A series of seven drop structures were constructed to prevent channel incision and protect the RYTW. The CKW was constructed upstream and should repeat a similar scenario of channel change as in the RYTW.

Stage 4 illustrates the channel conditions of recent years. The channel is temporarily stable because of the drop structure function, and the failure of the WHLB drop structure caused the WHLB collapse. The knickpoint of the WHLB migrated rapidly and vanished upstream. The local erosion in the downstream area of the CKW is the dominant factor in the upstream region of the study reach.

5.2. Possible future channel evolution

The Renyitan Weir intakes water to the Renyitan Reservoir, which is the most important water resource for Chiayi County. Although the deeply incised valley channel is extremely unfavorable for the stability of the RYTW, the weir must maintain the function of water extraction until a replacement is prepared. Currently, the channel downstream of RYTW is temporarily stable because of the grade control from the drop structures, whereas the local scour and erosion of the downstream extension are still active at the CKW. In the lateral direction of the channel, the process of channel widening is slow but ongoing. The channel widening is able to increase the channel capacity but might endanger the structure stability. However, the adjustment of channel geometry will also be influenced by the magnitude of future floods. Once any of the drop structures downstream of the RYTW are destroyed from flooding, the knickpoint migration could again induce rapid erosion and threaten the stability of the structures upstream.

From the studies of dam removal, the dominant factors affecting the succeeding channel evolution may include sediment characteristics and distribution, basin hydrology and sediment yield, valley configuration, knickpoint form, and dam removal timeline (Cannatelli and Curran, 2012; Sawaske and Freyberg, 2012; Tullos and Wang, 2014). Most of the factors are similar in the WHLB and RYTW because the two sites are within 3 km. Based on the experience of the WHLB failure, the channel will readjust to a smooth slope if the RYTW is removed (either by floods or for the purposes of future environmental restoration). Because the height of the knickpoint in the RYTW is approximately twice as large as the knickpoint in the WHLB, if the RYTW is removed, then the adjusted channel length will be much longer than it would be for a WHLB failure.

5.3. The lessons learned from the case

Resistant rocks generally set the base level for landscape boundaries (Whipple, 2004). However, the rapid erosion of weak or soft rock is not unusual over several streams that flow through the Western Foothills geological province of Taiwan (Lai et al., 2011; Huang et al., 2013b; Liao et al., 2013). The annual erosion rate of soft rock could be over ten meters in a vertical direction and a hundred meters with respect to knickpoint migration (Huang et al., 2013b).

Rapid channelization and bedrock incision caused the failure or damage of engineering facilities in the study reach over the study period. In total, five bridges have been destroyed by floods since 1988 (listed in Table 1). Four out of the five bridge failures were caused by scouring of the pile foundation because of an unexpected magnitude of bedrock incisions; the Wufeng Bridge failure occurred because the overflow broke the levees and destroyed the abutment. The lateral structures, including the weirs and drop structures, also suffered substantial damage from the rapid bedrock incision. The local scour of the lateral structure undermined the toe of the foundations and threatened the stability of the structures, which induced failure at several drop structures. Inevitable repairs for the lateral structures are required to maintain their function, especially for the Renyitan Weir and Chukou Weir. However, it is not economical to exhaustively repair the structures periodically. In addition to impacting the major structures, channel incisions have lowered the bed elevation and level of the stream flow. The original diversion works for irrigation lost their ability to extract water from the lower water levels using gravity flow. Moreover, the decreased water level in the river channel has lowered the ground water table and could create certain unexpected problems, such as ground subsidence adjacent to the river.

The soft bedrock erosion changes in channels are unidirectional and might not stop once initiated. Lateral or longitudinal structures constructed at a site with underlying soft rock should avoid the likelihood of armor layer loss and activation of bedrock erosion. Once the bedrock erosion is initiated, the erosion process is irreversible. Thus, a designer should be especially aware of the need to dissipate the excess energy that is induced.

If the stream power cannot be controlled, the drop structures that are constructed in the soft bedrock channels will not be stable for the long term. Huang et al. (2013a) suggested three possible causes for the structural instability in the five cases of drop structure failure. The three possible causes include the rapid rate of local scour, scouring at the interface of the artificial material and soft rock, and impact from large boulders. An economic and effective design of countermeasures for preventing local scour that considers the possible failure mechanisms related to soft rock erosion should be developed.

Moreover, the severe changes in channel morphology in this case suggest that sediment mining should be prevented in sites with a thin layer of sediment that underlies the soft rock. If the construction of a weir is required, the following strategies should be considered: 1) select a site with suitable geology conditions (e.g., massive cemented sandstone is relatively more resistant than mudstone) through careful geological investigation; 2) utilize water control gates such as drum gates or rubber dams to minimize the head difference during large floods through the controlling operation; and 3) select a site with a wide cross section to minimize the increase of stream power as a result of a diminished channel from the weir structures. These strategies may also be considered for preventing intense soft bedrock erosion caused by other lateral structures. However, more site-specific conditions should be explored in the engineering design.

6. Conclusions

A variety of engineering works are constructed in streams for flood control and water resource purposes, and human engineering projects and instream gravel mining significantly alter the natural adjustments of river systems and cause the evolution of channel morphologies. Compared to river beds composed of resistant rock, the significant incision of river channels on a weak or soft rock is possible and merits concern from the engineering sector. In the present study, the Bachang River in southwestern Taiwan is an example that demonstrates channel evolution that results from human activity. This study presents the lessons learned from the inducement of engineering problems, and the following conclusions can be drawn from this case study.

1. The processes of channel evolution are divided into four consecutive stages that are triggered by gravel mining and various structures.
2. The causes of channel change include six factors from the two categories: natural factors, such as geological conditions, hydrological conditions, and the processes of bedrock erosion; and human factors, such as gravel mining, lateral structures, and levees.
3. Prior to human disturbance, the river channel in the studied reaches of the Bachang River had remained a braided alluvial type, but

human activity changed the alluvial-type channel to a gorge-type channel over several short decades. The dominance of human impacts on the change in river morphology in this case study appears to be evident.

4. The maximum accumulated depth of the channel incision is approximately 30 m with an average annual incision rate at the meter scale. The maximum width decreases to one-sixth of the original within a century, and an equivalent rate of magnitude and width change is rarely observed worldwide.
5. Once the soft rocks are exposed on the riverbed without the protection of an armoring layer, the erosion process is rapid and unceasing. Substantial typhoon flooding has significantly enhanced the bedrock erosion process.
6. The impact of lateral structures (e.g., weirs and grade controls) and longitudinal structures (e.g., levees) on the channel incision vary. The levee has more impacts at the early stages of channel incision, whereas the local scour of weirs contributes to channel incision as long as the weir exists.
7. For a lateral or longitudinal structure to be constructed on a site with underlying soft rocks, it is advisable to avoid losing the armor layer and activating bedrock erosion. Once bedrock erosion is initiated, the erosion process might be irreversible. Several bridges and grade control structures in western Taiwan are examples of structures that have been destroyed by typhoon floods.

Acknowledgments

The work presented in this paper was made possible through the support of the Water Resources Planning Institute, Water Resources Agency, Ministry of Economic Affairs, Taiwan (140000 USD), and by the National Science Council (Project nos. NSC 101-2625-M-009-009 and NSC 101-2625-M-009-012). The authors would also like to express their appreciation for the helpful comments from the anonymous reviewers and editor; their comments have significantly improved this paper.

References

Bollaert, E., Schleiss, A., 2003. Scour of rock due to the impact of plunging high velocity jets part I: a state-of-the-art review. J. Hydraul. Res. 41, 451–464.

Cannatelli, K.M., Curran, J.C., 2012. Importance of hydrology on channel evolution following dam removal: case study and conceptual model. J. Hydraul. Eng. ASCE 138, 377–390. http://dx.doi.org/10.1061/(asce)hy.1943-7900.0000526.

Chang, H.W., Tien, Y.M., Juang, C.H., 1996. Formation of south-facing bald mudstone slopes in southwestern Taiwan. Eng. Geol. 42, 37–49. http://dx.doi.org/10.1016/0013-7952(96)00066-X.

Cheng, M.-H., Liao, J.-J., Pan, Y.-W., Li, G.-W., Huang, M.-W., Lo, W.-H., Hsu, S.-T., 2010. Soft-rock scouring processes downstream of weirs. In: Burns, S.E., Bhatia, S.K., Avila, C.M.C., Hunt, B.E. (Eds.), International Conference on Scour and Erosion (ICSE-5), San Francisco, California, United States, pp. 724–733.

Dadson, S.J., Hovius, N., Chen, H., Dade, W.B., Hsieh, M.-L., Willett, S.D., Hu, J.-C., Horng, M.-J., Chen, M.-C., Stark, C.P., Lague, D., Lin, J.-C., 2003. Links between erosion, runoff variability and seismicity in the Taiwan orogen. Nature 426, 648–651. http://dx.doi.org/10.1038/nature02150.

Dewitte, O., Jasselette, J.C., Cornet, Y., Van Den Eeckhaut, M., Collignon, A., Poesen, J., Demoulin, A., 2008. Tracking landslide displacements by multi-temporal DTMs: a combined aerial stereophotogrammetric and LIDAR approach in western Belgium. Eng. Geol. 99, 11–22. http://dx.doi.org/10.1016/j.enggeo.2008.02.006.

Downs, P.W., Dusterhoff, S.R., Sears, W.A., 2013. Reach-scale channel sensitivity to multiple human activities and natural events: Lower Santa Clara River, California, USA. Geomorphology 189, 121–134. http://dx.doi.org/10.1016/j.geomorph.2013.01.023.

Gregory, K.J., 2006. The human role in changing river channels. Geomorphology 79, 172–191. http://dx.doi.org/10.1016/j.geomorph.2006.06.018.

Hooke, J.M., 2006. Human impacts on fluvial systems in the Mediterranean region. Geomorphology 79, 311–335. http://dx.doi.org/10.1016/j.geomorph.2006.06.036.

Huang, M.-W., Liao, J.-J., Pan, Y.-W., Cheng, M.-H., 2013a. Failure processes of the vertical drop structures in weak bedrock channel. The 23rd International Ocean and Polar Engineering Conference (ISOPE-2013), Anchorage, Alaska, USA.

Huang, M.-W., Pan, Y.-W., Liao, J.-J., 2013b. A case of rapid rock riverbed incision in a coseismic uplift reach and its implications. Geomorphology 184, 98–110. http://dx.doi.org/10.1016/j.geomorph.2012.11.022.

Hung, J.H., Wiltschko, D.V., Lin, H.C., Hickman, J.B., Fang, P., Bock, Y., 1999. Structure and motion of the southwestern Taiwan fold and thrust belt. Terr. Atmos. Ocean. Sci. 10, 543–568.

Kondolf, G.M., 1994. Geomorphic and environmental — effects of instream gravel mining. Landsc. Urban Plan. 28, 225–243.

Kondolf, G.M., 1997. Hungry water: effects of dams and gravel mining on river channels. Environ. Manag. 21, 533–551. http://dx.doi.org/10.1007/s002679900048.

Lai, Y.G., Greimann, B.P., Wu, K.W., 2011. Soft bedrock erosion modeling with a two-dimensional depth-averaged model. J. Hydraul. Eng. ASCE 137, 804–814. http://dx.doi.org/10.1061/(ASCE)HY.1943-7900.0000363.

Lane, E.W., 1955. The importance of fluvial morphology in hydraulic engineering. Proc. Am. Soc. Civ. Eng. 81, 1–17.

Lane, S.N., 2000. The measurement of river channel morphology using digital photogrammetry. Photogramm. Rec. 16, 937–957. http://dx.doi.org/10.1111/0031-868x.00159.

Lee, D.H., Tien, K.G., Juang, C.H., 1996. Full-scale field experimentation of a new technique for protecting mudstone slopes, Taiwan. Eng. Geol. 42, 51–63. http://dx.doi.org/10.1016/0013-7952(95)00063-1.

Li, Y.H., 1976. Denudation of Taiwan island since Pliocene epoch. Geology 4, 105–108.

Liao, C.-T., Yeh, K.-C., Huang, M.-W., 2013. Development and application of 2-D mobile-bed model with bedrock river evolution mechanism. J. Hydro Environ. Res. http://dx.doi.org/10.1016/j.jher.2013.03.001.

Liebault, F., Piegay, H., 2002. Causes of 20th century channel narrowing in mountain and piedmont rivers of southeastern France. Earth Surf. Process. Landf. 27, 425–444. http://dx.doi.org/10.1002/esp.328.

Liu, T.-K., 1982. Tectonic implication of fission track ages from the Central Range, Taiwan. Proc. Geol. Soc. China 25, 22–37.

Reid, L.M., 1993. Research and cumulative watershed effects. General Technical Report PSW-GTR-141. Pacific Southwest Research Station, Forest Service, U.S. Department of Agriculture, Albany, CA.

Rosgen, D., 1996. Applied river morphology. Wildlife Hydology, Pagosa Springs, Colorado.

Sawaske, S.R., Freyberg, D.L., 2012. A comparison of past small dam removals in highly sediment-impacted systems in the U.S. Geomorphology 151, 50–58. http://dx.doi.org/10.1016/j.geomorph.2012.01.013.

Schiefer, E., Gilbert, R., 2007. Reconstructing morphometric change in a proglacial landscape using historical aerial photography and automated DEM generation. Geomorphology 88, 167–178. http://dx.doi.org/10.1016/j.geomorph.2006.11.003.

Schumm, S.A., 1979. Geomorphic thresholds — concept and its applications. Trans. Inst. Br. Geogr. 4, 485–515. http://dx.doi.org/10.2307/622211.

Simon, A., Rinaldi, M., 2006. Disturbance, stream incision, and channel evolution: the roles of excess transport capacity and boundary materials in controlling channel response. Geomorphology 79, 361–383. http://dx.doi.org/10.1016/j.geomorph.2006.06.037.

Stock, J.D., Montgomery, D.R., Collins, B.D., Dietrich, W.E., Sklar, L., 2005. Field measurements of incision rates following bedrock exposure: implications for process controls on the long profiles of valleys cut by rivers and debris flows. Geol. Soc. Am. Bull. 117, 174–194. http://dx.doi.org/10.1130/b25560.1.

Surian, N., Rinaldi, M., 2003. Morphological response to river engineering and management in alluvial channels in Italy. Geomorphology 50, 307–326. http://dx.doi.org/10.1016/S0169-555X(02)00219-2.

Tinkler, K.J., Wohl, E.E., 1998. A primer on bedrock channels. In: Tinkler, K.J., Wohl, E.E. (Eds.), River Over Rock: Fluvial Processes in Bedrock Channels. American Geophysical Union, Washington DC, pp. 1–18.

Tullos, D., Wang, H.W., 2014. Morphological responses and sediment processes following a typhoon-induced dam failure, Dahan River, Taiwan. Earth Surf. Process. Landf. 39, 245–258. http://dx.doi.org/10.1002/esp.3446.

Whipple, K.X., 2004. Bedrock rivers and the geomorphology of active orogens. Annu. Rev. Earth Planet. Sci. 32, 151–185. http://dx.doi.org/10.1146/annurev.earth.32.101802.120356.

WRA (Water Resources Agency), 1967–2011. Hydrological Year Book of Taiwan. Water Resource Agency, Taichung, Taiwan (at http://gweb.wra.gov.tw/wrhygis/. (in Chinese)).

WRA (Water Resources Agency), 1990. Regulation Plan of the Bachang River — From the Chukou Bridge to Estuary. Water Resource Agency, Taichung, Taiwan (in Chinese).

WRA (Water Resources Agency), 2006. Study on Control Plan in the Downstream Scour Channel Section of Renyitan Weir in the Bachang River. Water Resource Agency, Taichung, Taiwan (in Chinese).

WRA (Water Resources Agency), 2011. Report on Review of Regulation Plan of Bachang River. Water Resource Agency, Taichung, Taiwan (in Chinese).

Wu, C.C., Kuo, Y.H., 1999. Typhoons affecting Taiwan: current understanding and future challenges. Bull. Am. Meteorol. Soc. 80, 67–80. http://dx.doi.org/10.1175/1520-0477(1999)080<0067:tatcua>2.0.co;2.

Yu, S.B., Chen, H.Y., 1998. Strain accumulation in southwestern Taiwan. Terr. Atmos. Ocean. Sci. 9, 31–50.

Zawiejska, J., Wyzga, B., 2010. Twentieth-century channel change on the Dunajec River, southern Poland: patterns, causes and controls. Geomorphology 117, 234–246. http://dx.doi.org/10.1016/j.geomorph.2009.01.014.